

Observation of perpendicular exchange bias in [Pd/Co]-CoO nanostructures: Dependence on size, cooling field, and training

Ildico L. Guhr,^{1,*} Olav Hellwig,² Christoph Brombacher,¹ and Manfred Albrecht^{1,†}

¹*Department of Physics, University of Konstanz, 78457 Konstanz, Germany*

²*Hitachi Global Storage Technologies, San Jose Research Center, 3403 Yerba Buena Road, San Jose, California 95135, USA*

(Received 16 May 2007; revised manuscript received 20 July 2007; published 30 August 2007)

Magnetic [Pd/Co] multilayer structures deposited onto self-assembled particle monolayers were capped with a CoO layer to study the size dependence of perpendicular exchange bias. Compared to the continuous film, the biased caps develop an asymmetric hysteresis loop and show a significantly higher exchange bias field and coercivity strongly depending on the cooling field and number of field cycles. The magnitude of the exchange bias field increases substantially as we scale down the particle diameter. Moreover, in contrast to the film, the coercivity exhibits a nonmonotonic temperature behavior with a local maximum at about 250 K, which may originate from strong spin fluctuations in the antiferromagnet.

DOI: [10.1103/PhysRevB.76.064434](https://doi.org/10.1103/PhysRevB.76.064434)

PACS number(s): 75.70.-i, 68.65.Ac, 75.75.+a, 77.80.Dj

I. INTRODUCTION

The development of advanced lithography tools for controlled fabrication of magnetic nanostructures has triggered new studies regarding the physical understanding of coupling phenomena and scaling behavior. In this regard, coupling phenomena such as exchange bias become particular complex when laterally patterned on the nanometer scale. The phenomenology of the exchange bias effect¹ occurring in materials composed of ferromagnetic (F) and antiferromagnetic (AF) interfaces has been extensively described in various review articles.²⁻⁴ The physical origin of exchange bias is generally accepted to be the exchange coupling between the AF and F components at the interface. The microscopic way this coupling translates into exchange bias is more controversial and many models have been proposed.^{2,5-8} The main characteristic of the existence of exchange bias is the shift of the hysteresis loop H_E along the field axis after field cooling from above the blocking temperature T_B of the system. Accompanying the loop shift are other related properties. Probably the most common is an increase of the coercivity (H_C , the zero-moment half-width of the hysteresis loop) below the Néel temperature T_N of the AF after a field cooling procedure.

Although there are many reports on exchange-biased nanostructures (see review article²), mainly with a ferromagnetic in-plane easy axis, very few of them address the effects of miniaturization on the exchange bias properties,⁹⁻¹³ where novel effects set in at some critical length scales. In this regard, self-assembled monolayers of monodisperse particles can be employed as a deposition mask for nanostructure fabrication. This approach has been used to study the exchange bias effect in nanostructures formed in the interstices after mask removal.¹⁴ Alternatively, the initial particle array can also be directly used as a topographic pattern. Co/Pd or Co/Pt multilayer deposition onto the particle array results in the formation of exchange-isolated magnetic caps.^{15,16} These so-formed arrays of ferromagnetic caps provide a template over large surfaces for studying the scaling behavior of exchange bias in magnetic nanostructures as recently demonstrated for the system [Pt/Co]-IrMn.¹³

In this paper, we have investigated the size-dependent scaling of the exchange bias properties in magnetic nanostructures with an out-of-plane easy axis obtained by depositing [Pd/Co]₃/CoO layers onto an array of spherical nanoparticles. In contrast to the [Pt/Co]-IrMn system,¹³ a strong perpendicular exchange bias effect was found. The evolution of coercivity H_C and exchange bias field H_E after field cooling in a negative field to different temperatures was studied for various cap sizes and cooling fields and compared to the behavior of the continuous film. These effects depend strongly on the number of loop cycles, the so-called training effect. In addition, the distribution of the blocking temperature was determined by applying a second field cooling procedure under a positive field following the method reported in Refs. 12 and 18.

II. EXPERIMENTAL DETAILS

For our study, we employed densely packed polystyrene particle arrays with a diameter d varying from 58 to 320 nm, which were obtained by self-assembly under slow evaporation of a solvent.¹⁹ These particle monolayers were capped with a magnetic film by dc magnetron sputtering in a 3 mTorr Ar atmosphere at room temperature. We deposited a Ta(15 Å)/Pd(30 Å) buffer layer system followed by a multilayer stack composed of two bilayers of [Co(5 Å)/Pd(20 Å)]. The film was subsequently capped with an additional 15-Å-thick Co layer and exposed to ambient atmosphere, where about 10 Å of the Co film oxidize to CoO.²⁰ This natural oxide of Co is a high anisotropy AF and can conveniently be used to exchange bias the Pd/Co multilayer below. In comparable film structures, a strong perpendicular exchange bias effect was reported.²⁰ Finally, the sample was covered with an additional 20-Å-thick Pd layer to prevent further oxidation. For comparison, a continuous film was simultaneously deposited on a plain glass substrate. Due to the limited oxidation thickness, which is smaller than the total thickness of the Co layer, a quite homogeneous radial CoO layer thickness across the particle surface is expected. This is in contrast to the F layer, where the thickness

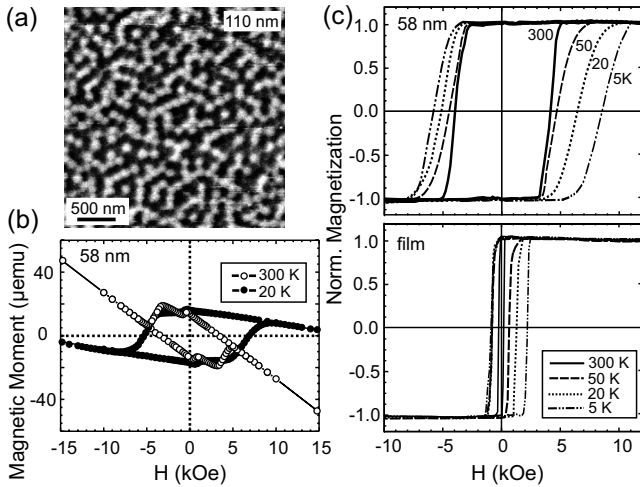


FIG. 1. (a) MFM image of a magnetic cap array with 110 nm particles at room temperature. (b) M - H loop for $[\text{Pd}/\text{Co}]_3\text{-CoO}$ caps with a size of 58 nm measured at 20 and 300 K, including the magnetic contributions of the substrate and film areas which were initially not covered by particles. (c) Reduced M - H loops revealing the reversal of the 58 nm cap array at various temperatures and for a continuous film which was prepared under the same conditions.

is reduced from the top center of the particles toward the outer parts of each sphere. In addition, the F caps exhibit a locally varying anisotropy orientation pointing perpendicular to the particle surface,^{15,16} forming a rather complex F-AF nanoscale system.

The magnetic characterization was carried out using magnetic force microscopy (MFM), polar magneto-optical Kerr effect (MOKE), and superconducting quantum interference device (SQUID) magnetometry.

III. RESULTS AND DISCUSSION

A. Switching field distribution and asymmetry

A MFM image of a capped 110 nm particle array was taken at room temperature in the demagnetized state [Fig. 1(a)]. The F cap structures revealed a quasi-single-domain state at remanence for all sizes indicated by a uniform dark or bright island contrast with an averaged magnetization orientation pointing up or down, respectively, similar to results reported earlier.^{15,16} The samples were characterized by SQUID magnetometry measurements applying the field perpendicular to the substrate plane. Typical out-of-plane SQUID hysteresis loops of the smallest F/AF caps grown onto 58 nm particles are presented in Fig. 1(b), which were measured at room temperature and 20 K after field cooling at -50 kOe. Due to areas which are not covered by particles, a small continuous film contribution is superimposed in the hysteresis loops as indicated by the low field reversal step. In addition, a strong diamagnetic contribution from the glass substrate contributes to the total moment. However, these individual contributions can be well separated and also identified by MOKE investigations. It is worth noting that we do not see a contribution from the material deposited into the interstices formed by the particle array, which can be ex-

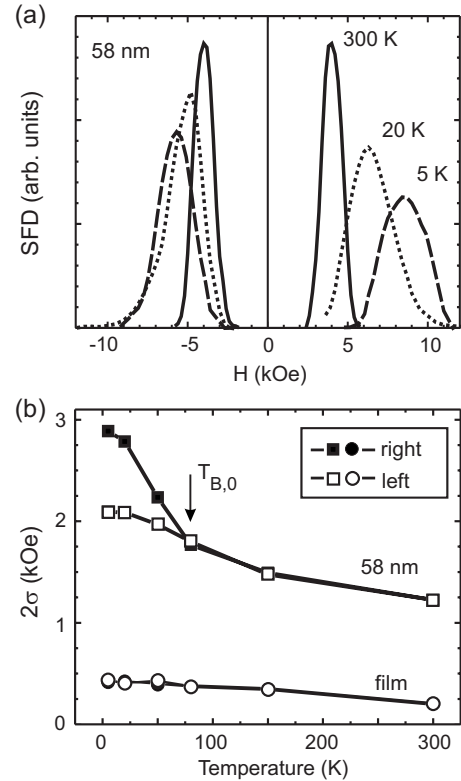


FIG. 2. (a) Switching field distribution (SFD) of the 58 nm cap array and (b) corresponding width of the distribution including results for the continuous film for various temperatures as extracted from the hysteresis loops presented in Fig. 1(c). Note that the error bars are smaller than the symbol size.

plained by the deposition geometry. One sputter gun (Pd) is on axis, while the other (Co) is off axis and tilted, and to improve the homogeneity of the deposited film stack the sample is rotating during deposition. Therefore, shadowing effects of the particles prevent to a large extent Co from being deposited into the interstices.

In Fig. 1(c), the reduced hysteresis loops of the 58 nm caps (corrected for the continuous film and diamagnetic contributions) and of the continuous film are presented for various temperatures. While the continuous film displays a hysteresis loop shift H_E of 0.7 kOe and coercivity H_C of 1.6 kOe at 5 K, the nanocaps exhibit much larger values, namely, 1.4 and 7.2 kOe, respectively. However, the loop shift occurs in both samples at about 80 K, indicating the blocking temperature T_B of the system. Note that we observe a negative exchange bias, although the loop shift is positive. In contrast to conventional practice, in our study a negative cooling field was applied.

The individual hysteresis loops were further analyzed concerning the switching field distribution (SFD) on both branches, given by the derivative of M versus H . Figure 2(a) shows the SFD of the 58 nm particle caps. The SFD becomes broader with decreasing temperature but is on both branches more or less identical. However, this situation changes at temperatures below the blocking temperature. Here, the width of the SFD for the ascending branch increases much stronger than for the descending branch. The extracted SFDs

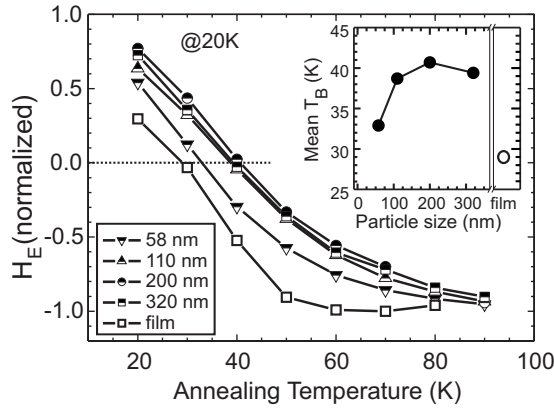


FIG. 3. Exchange bias field (normalized to the initial H_E value at 20 K) as a function of annealing temperature. H_E vanishes at slightly different annealing temperatures indicating the mean blocking temperature as summarized in the inset.

were further fitted by a Gaussian function to obtain a measure of the width of the distribution, given by the standard deviation σ . As can be seen in Fig. 2(a), the extracted distributions are not completely symmetric, but as a first approximation a Gaussian function is sufficient to describe the functional behavior of the temperature dependence. The 2σ values of the SFD for both branches are plotted in Fig. 2(b) summarizing the results. This asymmetry in the loops is well known in the literature, in particular, for CoO systems,^{21–23} and has recently been demonstrated to be an intrinsic effect of exchange bias.²⁴ While an asymmetric behavior was observed for all particle sizes, the continuous film revealed almost no asymmetry in the SFD [see Fig. 2(b)]. However, it has been shown that the occurrence of an asymmetry depends on the angle between magnetic field and easy axis of the antiferromagnet,²⁵ a feature which is strongly pronounced in the cap structures, where different angles between the applied field and the anisotropy axis are present.^{15,16}

Note that there are certainly dipolar interactions that broaden the intrinsic SFD, and they become larger as we scale down the nanosphere size.¹⁷ However, they should be symmetric with respect to the SFD and should have no impact on the bias.

B. Blocking temperature distribution

The onset temperature of exchange bias is quite similar throughout the whole series. However, in particular, for the smallest particles one might expect the nanostructures to be more prone to thermal activation due to the reduced coordination of the spins located at the outer parts of the spheres, resulting in a reduced bias field in the caps. The blocking temperature distribution of the various samples was determined by field cooling the samples under a positive field (+50 kOe) from different annealing temperatures after the standard cooling procedure in a negative field (−50 kOe) down to 20 K following the method reported in Refs. 12 and 18. Figure 3 shows the exchange bias field H_E measured at 20 K as a function of the annealing temperature from which

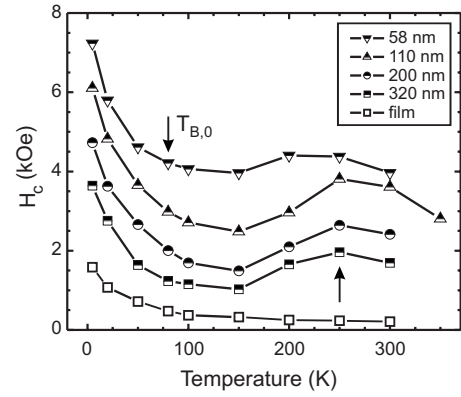


FIG. 4. Temperature dependence of the coercivity measured for various particle sizes and for the continuous film.

the samples have been field cooled in the positive field. With increasing annealing temperature, the value of the exchange bias field (normalized to the initial H_E value at 20 K) is reduced, changes sign, and approaches its initial value. The relative change in bias field is due to CoO regions with local blocking temperatures lower than the annealing temperature; thus, these regions are reversed during the second annealing procedure when field cooled. Note that the value for the exchange bias at an annealing temperature of 20 K is already reduced due to the onset of thermal activation, even at 20 K. As summarized in the inset of Fig. 3, H_E vanishes at slightly different annealing temperatures at about 40 K for the larger particles and at about 33 K for the smallest particle size, indicating a lower thermal stability. In contrast, in the continuous film the zero crossing occurs at an even lower temperature of 29 K, revealing a somewhat sharper distribution.

C. Coercivity and exchange bias

The variation of the coercivity as function of temperature and particle size is summarized in Fig. 4 and compared to the continuous film properties. Each individual hysteresis loop was measured after room temperature annealing followed by field cooling at −50 kOe. The coercivity of the cap structures increases with decreasing particle size and is much larger than the one measured for the continuous film. However, while the film exhibits a steady increase in coercivity with decreasing temperature, in particular, below T_B , the coercivity of the caps passes through a broad local maximum at about 250 K for all particle sizes. Similar effects have been observed in other thin film systems and also appear in some theoretical models,^{26–28,30} where the existence of the peak in coercivity is due to the onset of AF spin ordering followed by an increase of its anisotropy as the Néel point is approached from higher temperatures. However, as the Néel temperature is expected to be much lower in our system, it is suggested that the increase of spin fluctuations in the AF leads to an enhancement in the uniaxial anisotropy of the F, and therefore results in an enhanced coercivity above the Néel temperature as proposed by Leighton *et al.*³¹ Note that the expected reduction in Néel temperature as observed in thin CoO films³² might be even more pronounced in the cap

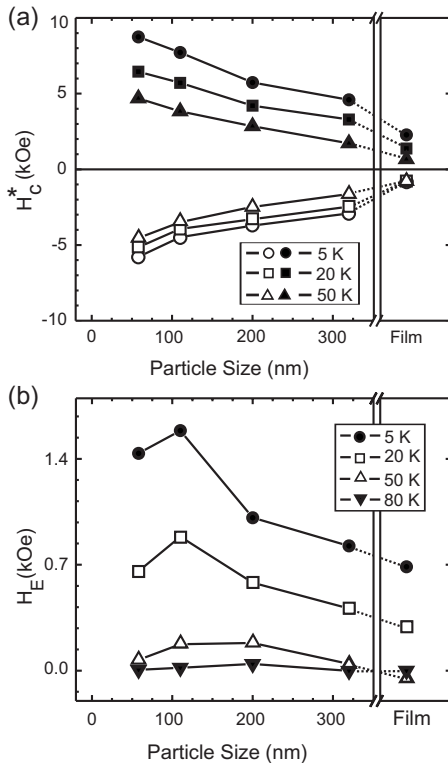


FIG. 5. (a) Temperature dependence of the branch coercivity H_C^* and (b) resulting exchange bias field measured for various particle sizes and for the continuous film.

structures due to limited size and local variations in CoO thickness. Another feature is the strong enhancement in coercivity below the blocking temperature, which is usually linked to the anisotropy distribution present in the AF layer.³⁰

The evolution of the coercivity for the negative and positive branches is presented in Fig. 5(a) for various temperatures below T_B as a function of particle size. The continuous film, which is also included in Fig. 5(a), shows a pronounced temperature dependence of the coercivity at the positive branch, while the negative branch is almost unchanged. The cap structures reveal on both branches a strong coercivity variation with temperature, which increases almost linearly with decreasing temperature and particle size. The corresponding loop shifts H_E are summarized in Fig. 5(b). The cap structures show a strong enhancement in loop shift for all sizes which increases with reducing the cap size except for the smallest particles of 58 nm, where a slight drop in exchange bias is observed. For the continuous film, the exchange bias sets in slightly below 80 K and between 50 and 20 K a change in the direction of the exchange bias effect was observed, changing from positive to negative, an effect that has also been observed in other thin film systems.³³ Lower temperatures result in a steady increase of the exchange bias field.

There are several effects that might contribute to the enhancement of the exchange bias field of the cap structures. First, there is certainly a difference in the morphology of the films grown on top of the curved surface of the polystyrene spheres and the continuous film grown on a glass substrate.

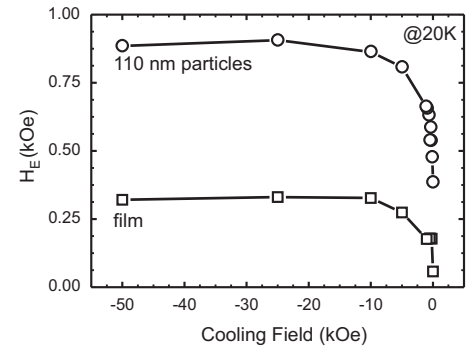


FIG. 6. Dependence of H_E on the strength of the cooling field measured after saturation and field cooling from room temperature down to 20 K for the 110 nm cap array and the continuous film.

Scanning tunneling microscopy studies of Co/Pd multilayer films grown on polystyrene spheres have revealed a film morphology with grain sizes of about 6 nm independent of the sphere size and much smaller than observed for the continuous film.¹⁵ This could explain the enhanced H_E values of the nanostructures compared to the continuous film, since following the model of Takano *et al.*³⁴ smaller grains will lead to an increase of the exchange bias field. However, it does not explain an inverse proportionality between the exchange bias field and the particle size. Another contribution to the enhancement of H_E in the nanostructures might come from the local variation of the ferromagnetic layer thickness across the particle surface. The thickness of the F decreases from the top center of the sphere toward its edges. H_E will therefore increase along this direction as the exchange bias field is known to depend inversely proportional on the thickness of the ferromagnet.² In addition, based on Malozemoff's random field model,⁶ an inverse proportionality between the exchange bias field and the particle size might be expected.² This scaling was already observed for perpendicular Co/Pt-IrMn cap structures revealing a single-domain AF spin configuration.¹³ However, the deviation of this scaling behavior for the smallest particle size is not clear and probably linked to the lower thermal stability as indicated by a reduction in blocking temperature. Moreover, the cap structures provide an intrinsic variation of magnetic properties such as the anisotropy orientation in the F layer and the magnitude of the exchange coupling between F and AF layers across the caps which will certainly affect the magnetic properties.

D. Cooling field dependence

A variation of the cooling field allowed the study of the influence of its strength on the exchange bias field.²⁹ In order to start with the same initial magnetization state, the samples were all saturated at room temperature in a field of -50 kOe before field cooling down to 20 K in differently strong negative fields between 0 and -50 kOe. We initially observe a sharp increase in both H_E and H_C with increasing cooling field up to 1 kOe, followed by a more gradual saturation of this effect at higher cooling fields, as shown in Fig. 6 for the 110 nm particle array. Note that even for zero-field cooling, a

finite loop shift is obtained. This cooling field dependence might indicate that the spins causing the bias effect are not located at the F/AF interface. If they were at the interface, one would expect a nearly complete loop shift already at zero cooling field for samples that were saturated before cooling. AF interface spins are strongly exchange coupled to the F which always aligns for any cooling field (since we have full remanent magnetization in all samples), leading to a vanishing cooling field dependence. For the continuous film, we observe a similar cooling field dependence of H_E .

E. Training effect

As the AF layer on the caps exhibits multiple magnetic easy axes, inherent frustration of the spins at the interface along with certain symmetry of the AF anisotropies is expected to lead to an irreversible training effect. It has been shown that there are two types of training effects, one initial effect only occurring between the first and the second loop and another one also present in all subsequent loops but slowly decreasing in strength. The first type of training effect has been proposed to arise from the symmetry of the magnetic anisotropy in the AF layer.³⁰ For the second type of training effect, it has been demonstrated experimentally that, in thin film systems, the reduction of H_E with the number of loop cycles is often following a power law and arises from the reconfiguration of the AF moments or domains during the magnetization cycling.³⁵ Note that in our system, no AF domain walls are assumed, since only 4 monolayers of CoO are formed, and thus the concept of a domain wall seems inadequate because of its high magnetocrystalline anisotropy.⁵ The training effect was systematically investigated after field cooling from room temperature to 5 K in a field of -50 kOe for the cap arrays as well as for the continuous film. The presence of the two types of training effect indicated by a sharp drop in H_E and H_C for the second M - H loop followed by a slower decrease with increasing number of loop cycles was observed for all systems (Fig. 7). For the cap arrays, the relative training effect is not as pronounced as for the continuous film. The specific underlying microstructure of the cap morphology and magnetostatic interactions will play an important role in this observed training behavior.

In Ref. 35, a phenomenological approach is given based on the concept that the AF pinning system deviates from its ground state and approaches the latter on subsequent cycling. In this approach, the values for the exchange bias field are generated by the implicit expression

$$H_E(n+1) = H_E(n) - \alpha[H_E(n) - H_E^e]^3, \quad (1)$$

where n gives the number of cycles, α is a system dependent constant, and H_E^e is the exchange bias field in the limit of infinite loops. As shown in Fig. 7, for the example of the continuous film, this universal two-parameter approach can be used to describe our data.

IV. CONCLUSION

In conclusion, we have demonstrated the possibility of inducing large perpendicular exchange bias in Pd/Co-CoO

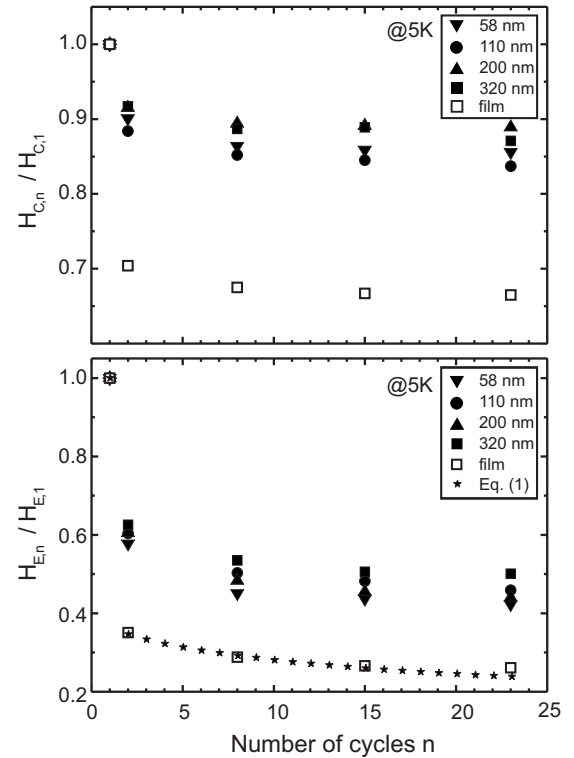


FIG. 7. Variation of the coercivity and exchange bias field with increasing number of loop cycles measured at 5 K for a number of various cap arrays and for the continuous film. In the lower graph, values calculated for the continuous film [Eq. (1), $\alpha=0.919$, $H_E^e=0.108$] following Ref. 35 are included.

nanostructures employing self-assembled nanoparticle arrays. Thereby, the magnitude of the exchange bias depends strongly on the applied cooling field and shows a substantial training effect. It is found that the magnitude of the coercivity of both hysteresis branches increases strongly as the cap size is reduced accompanied by an asymmetry of the SFD below the blocking temperature, which in turn shows only weak size dependence. In addition, a nonmonotonic temperature dependence of the coercivity was found which might be connected with strong spin fluctuations in the AF. In order to get a better understanding of how the curvature of the particle affects the film morphology of the AF and F and thus their interaction, it would be very interesting to compare in a future study planar nanostructures grown on a prepatterned substrate with nanostructures grown on spherical particles. The reported phenomena may help further implement exchange-biased nanostructures into magnetic nanodevices.

ACKNOWLEDGMENTS

The authors would like to thank J. Boneberg, G. Schatz (University of Konstanz), and E. E. Fullerton (UC San Diego) for fruitful discussions. This work was supported by the German Science Foundation (DFG) through the Emmy-Noether program and the European project *MAFIN* (Contract No. FP6-26513) at the University of Konstanz.

*ildico.luise.guhr@uni-konstanz.de

[†]Present address: Institute of Physics, Chemnitz University of Technology, 09107 Chemnitz, Germany.

- ¹W. H. Meiklejohn and C. P. Bean, *Phys. Rev.* **105**, 904 (1957).
- ²J. Nogués, J. Sort, V. Langlais, V. Skumryev, S. Suriñach, J. Muñoz, and M. Baró, *Phys. Rep.* **422**, 65 (2005).
- ³J. Nogués and I. K. Schuller, *J. Magn. Magn. Mater.* **192**, 203 (1999).
- ⁴J. F. Bobo, L. Gabillet, and M. Bibes, *J. Phys.: Condens. Matter* **16**, S471 (2004).
- ⁵D. Mauri, H. C. Siegmann, P. S. Bagus, and E. Kay, *J. Appl. Phys.* **62**, 3047 (1987).
- ⁶A. P. Malozemoff, *Phys. Rev. B* **35**, 3679 (1987).
- ⁷U. Nowak, K. D. Usadel, J. Keller, P. Miltényi, B. Beschoten, and G. Güntherodt, *Phys. Rev. B* **66**, 014430 (2002).
- ⁸D. Suess, M. Kirschner, T. Schrefl, J. Fidler, R. L. Stamps, and J.-V. Kim, *Phys. Rev. B* **67**, 054419 (2003).
- ⁹J. Sort, B. Dieny, M. Fraune, C. Koenig, F. Lunnebach, B. Beschoten, and G. Güntherodt, *Appl. Phys. Lett.* **84**, 3696 (2004).
- ¹⁰V. Baltz, J. Sort, S. Landis, B. Rodmacq, and B. Dieny, *Phys. Rev. Lett.* **94**, 117201 (2005).
- ¹¹J. Eisenmenger, Z. P. Li, W. A. A. Macedo, and I. K. Schuller, *Phys. Rev. Lett.* **94**, 057203 (2005).
- ¹²A. Bollero, V. Baltz, B. Rodmacq, B. Dieny, S. Landis, and J. Sort, *Appl. Phys. Lett.* **89**, 152502 (2006).
- ¹³G. Malinowski, M. Albrecht, I. L. Guhr, J. M. D. Coey, and S. van Dijken, *Phys. Rev. B* **75**, 012413 (2007).
- ¹⁴J. Sort, H. Glaczynska, U. Ebels, B. Dieny, M. Giersig, and J. Rybczynski, *J. Appl. Phys.* **95**, 7516 (2004).
- ¹⁵T. C. Ulbrich, D. Makarov, G. Hu, I. L. Guhr, D. Suess, T. Schrefl, and M. Albrecht, *Phys. Rev. Lett.* **96**, 077202 (2006).
- ¹⁶M. Albrecht, G. Hu, I. L. Guhr, T. C. Ulbrich, J. Boneberg, P. Leiderer, and G. Schatz, *Nat. Mater.* **4**, 203 (2005).
- ¹⁷O. Hellwig, A. Berger, T. Thomson, E. Dobisz, H. Yang, Z. Bandic, D. Kercher, and E. E. Fullerton, *Appl. Phys. Lett.* **90**, 162516 (2007).
- ¹⁸S. Soeya, S. Nakamura, T. Imagawa, and S. Narishige, *J. Appl. Phys.* **77**, 5838 (1995).
- ¹⁹F. Burmeister, W. Badowsky, T. Braun, S. Wieprich, J. Boneberg, and P. Leiderer, *Appl. Surf. Sci.* **144-145**, 461 (1999).
- ²⁰S. Maat, K. Takano, S. S. P. Parkin, and E. E. Fullerton, *Phys. Rev. Lett.* **87**, 087202 (2001).
- ²¹E. Pina, C. Prados, and A. Hernando, *Phys. Rev. B* **69**, 052402 (2004).
- ²²O. Hellwig, S. Maat, J. B. Kortright, and E. E. Fullerton, *Phys. Rev. B* **65**, 144418 (2002).
- ²³F. Radu, M. Etzkorn, T. Schmitte, R. Siebrecht, A. Schreyer, K. Westerholt, and H. Zabel, *J. Magn. Magn. Mater.* **240**, 251 (2002).
- ²⁴J. Camarero, J. Sort, A. Hoffmann, J. M. García-Martín, B. Dieny, R. Miranda, and J. Nogués, *Phys. Rev. Lett.* **95**, 057204 (2005).
- ²⁵B. Beckmann, U. Nowak, and K. D. Usadel, *Phys. Rev. Lett.* **91**, 187201 (2003).
- ²⁶C. Leighton, M. R. Fitzsimmons, A. Hoffmann, J. Dura, C. F. Majkrzak, M. S. Lund, and I. K. Schuller, *Phys. Rev. B* **65**, 064403 (2002).
- ²⁷C. Leighton, J. Nogués, B. J. Jönsson-Åkerman, and I. K. Schuller, *Phys. Rev. Lett.* **84**, 3466 (2000).
- ²⁸C. Hou, H. Fujiwara, K. Zhang, A. Tanaka, and Y. Shimizu, *Phys. Rev. B* **63**, 024411 (2000).
- ²⁹B. Kagerer, C. Binek, and W. Kleemann, *J. Magn. Magn. Mater.* **217**, 139 (2000).
- ³⁰A. Hoffmann, *Phys. Rev. Lett.* **93**, 097203 (2004).
- ³¹C. Leighton, H. Suhl, M. Pechan, R. Compton, J. Nogués, and I. K. Schuller, *J. Appl. Phys.* **92**, 1483 (2002).
- ³²Y. J. Tang, D. J. Smith, B. L. Zink, F. Hellman, and A. E. Berkowitz, *Phys. Rev. B* **67**, 054408 (2003).
- ³³T. Gredig, I. N. Krivorotov, P. Eames, and E. D. Dahlberg, *Appl. Phys. Lett.* **81**, 1270 (2002).
- ³⁴K. Takano, R. H. Kodama, A. E. Berkowitz, W. Cao, and G. Thomas, *Phys. Rev. Lett.* **79**, 1130 (1997).
- ³⁵C. Binek, *Phys. Rev. B* **70**, 014421 (2004).